ChemComm

Accepted Manuscript

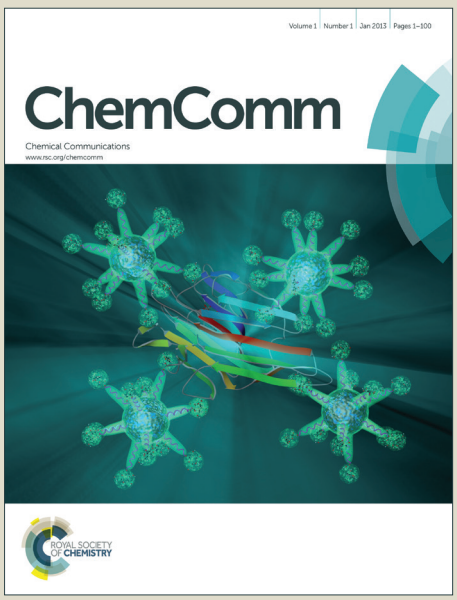

ROYAL SOCIETY OF CHEMISTRY

www.rsc.org/chemcomm

Journal Name

RSCPublishing

COMMUNICATION

Few layer graphene - supported palladium as highly efficient catalyst in oxygen reduction reaction

Cite this: DOI: 10.1039/xoxxoooooox

L. Truong-Phuoc,[a] C. Pham-Huu,[a] V. Da Costa[b] and I. Janowska[a*]

Received ooth January 2012,
Accepted ooth January 2012

DOI: 10.1039/xoxxoooooox

www.rsc.org/

New, active, stable and competitive to Pt catalysts are necessary for fuel cells development. Here, we present Few layer graphene - supported Pd revealing superior to Pt/C and Pd/C ORR performance (→ $E_{1/2}$ by 50 mV, ~ order magnitude ↑ I_{area} and I_{mass}, after 2500 cycles). The catalyst preparation is easily scalable, simple, inexpensive and eco-friendly.

Fuel cells are of great potential for energy production with a respect of environment protection; however the activation of sluggish oxygen reduction reaction (ORR) kinetic is a main obstacle in the enhancement of their efficiency and consequently their successful commercialization. Intensive efforts refer to a development of the active, stable and cost-attractive relatively to Pt ORR electrocatalyst; to its efficient synthesis and understanding of relation between structural/electronic features of the catalyst and its ORR property.[1,2] According to Sabatier's principle (intermediate catalyst-reactants binding strength) Pd is the closest Pt neighbor metal, but its ORR activity is usually few times lower than Pt;[3] though Pd is twice/three times cheaper and more abundant (0.015 ppm vs. 0.005 ppm Pt/all earth elements). A tuning of particles' structure rises different directions for Pt and Pd due to diversely size and facets dependent activity of both metals. Contrary to most active, small (~4 nm) and (111) facets Pt particles; the optimal current density and mass-specific activity for Pd particles are established for ≥ 16 nm and (100) facets.[4-6] The one order magnitude higher ORR activity of (100) enclosed Pd/C nanocubes compared to (111) rich octahedral Pd/C was attributed to lower poisoning of (100) facets by OH_{ad} in the acid medium and then higher exposition of reaction sites for O_2 adsorption.[5] The Pd (110) facets enriched Pd nanorods also showed a 10-fold higher ORR activity compared to Pd nanoparticles (and comparable to Pt/C) revealing the importance of structure-activity relationship.[7] Lower OH poisoning, and consequently higher activity of Pd are also generally observed in alkaline solution.[8] The principal modifications of Pd electronic structure as it is a case of Pt is alloying them with other metal (substrate) what, according to Nørskov, influences the surface reactivity by shifting of d-band center energies (ε_d) of metal.[9] Depending on the metal-metal (substrate) interaction, the position of d-band center shifts with amount of induced strain and/or the electronic distribution between metal and substrate (ligand effect, hybridization).[10-13,8] In this regard an enhanced activity and stability were measured, e.g. for Pd/Pt films,[8,12] or core shell type Pd/Pt NPs.[14-17] The enhanced activity was also observed for non-Pt, modified by Co and Fe Pd - supported nanoparticles in acid solution.[13] In alkaline solution, a flat Pd monolayer supported on Pt(111) exhibited $I_{k\,(0.9\,V)}$ four times higher than Pt(111) and positive potential shift by 50 mV in the kinetic-diffusion region; while an addition of Pd layers resulted in strong increasing of OH_{ad} coverage and lowering of activity.[11] Despite promising catalytic activity of Pd in alkaline solution, Wells et al. reported low stability of Pd/C during potential cycling.[18] The improved catalytic ORR performances of supported particles, both the activity and stability, were recently attained for Pt and Pt alloys by changing a standard carbon support to graphene; assigned to high electrical conductivity (high electron transfer) and chemical inertness of graphene compared to standard carbon.[1,19,20] Catalytically stable graphene supported FePt particles unrevealed six times higher activity than Pt/C.[21] The active non-metal iron phtalocyanine showed a superior stability than Pt once supported on N-doped graphene.[22] A superior stability was reported as well for N-doped graphene-Co_3O_4 hybrid in alkaline solution, where a comparable activity to Pt was attributed to the formation of an active interface.[23]

Here, we report on a new catalyst, few layer graphene supported Pd (Pd/FLG), unrevealing the best performance reported up to now among the monometallic supported catalysts in alkaline solution. Apart from high activity and stability, the preparation of both: FLG support and supported active phase is very attractive, which makes the Pd/FLG uncompetitive relatively to existing supported monometal catalysts. The FLG was previously prepared by easily scalable, high yield, eco-friendly and low cost method consisting of ultrasonic assisted -mechanical exfoliation of pencil lead (SI).[24,25]

Low resolution TEM micrographs (Fig.1A) show a relatively high dispersion of Pd on the FLG surface, while statistical TEM analysis

reveals rather trimodal distribution of particles with average size of ~3, 7 and 19 nm, and punctually larger particles of ~ 60 nm are observed (SI). According to HR-TEM, the Pd reveals heterogenous, more or less facet morphologies of smaller pyramidal- like (*z*-axis apex) and elongated nanorods- like particles (Fig. 1B, C, SI). The size and morphology discrepancy are probably related to variable local coalescence during reduction treatment. The particles coalesce depending on the distance between them, their initial size and their interaction with graphene, which, in turn, is affected by particles localization (well crystallized plane, defect-rich plane or edges of graphene). It was previously demonstrated by *in*-situ heating under TEM observations, that metal faceting and FLG edges are stabilizing factors for FLG-supported Pt particles at 400°C.[26] The HR-TEM and powder X-Ray diffraction analysis reveal the face-centered cubic (fcc) structure (Fig. 1). The fringes corresponding to (111) and (200) lattice spacing of fcc Pd respectively are distinguished in the HR-TEM micrograph and confirmed by corresponding peaks in XRD pattern. The overall Pd-Pd bond distance however seems to be lowered with a period varies from 0.0204 to 0.229 nm depending of particles' morphology (SI). The XRD-sharp peak at 27° (and 55°) confirms the presence of highly graphitized FLG support.

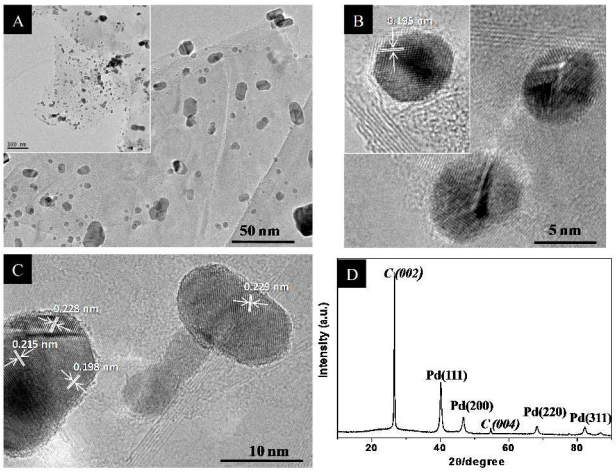

Figure 1. (A-C) Low and high magnification TEM micrographs and (D) XRD pattern of Pd/FLG catalyst.

AFM (Fig.2) and SEM (SI) characterizations show the existence of well separated pyramidal- or rods- like species and elongated structures which are punctually connected forming a kind of islands (Fig.2).

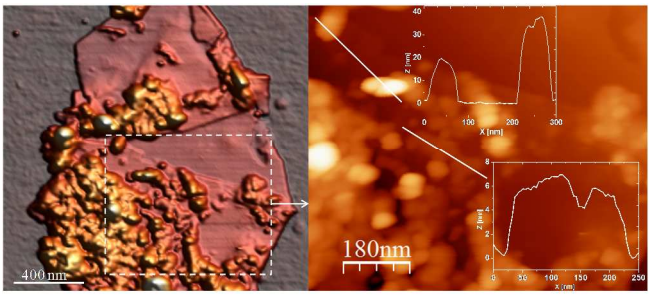

Figure 2. AFM image and profiles mapping of Pd/FLG catalyst.

Both types of structures are however flattened. The AFM "z" profiles performed on the largest particles (~ 60-80 nm) are in the range of 11-35 nm, where for planar structures they do not exceed 8 nm (Fig. 2, SI). In addition, the SEM shows that the highest "pyramidal-like" particles are in fact the planar aggregates of 2-3 flat Pd layers, which lateral size decreases in "z" direction from graphene surface (SI). The flattening of particles indicates important interaction between metal and graphene support.

The ORR property of Pd/FLG, together with the prepared Pd/C and state-of-art Pt/C as references were carried out in 0.1M KOH solution and rotating-(ring)-disk electrode (R(R)DE) method (SI). The Pd/FLG catalyst exhibits quite different characteristics in the cyclic voltammogram than Pt/C (SI). The main peak corresponding to OH^- adsorption in Pd/FLG is only slightly shifted toward lower potential, from ~ 0.79 (Pt) to ~ 0.75 V (Pd), with the presence of much weaker peak shifted to 0.6 V (Pd), which indicates only slightly higher OH^- coverage on Pd compare to Pt/C or Pd/C; e.g. this shift was much higher for earlier reported Pd layers deposited on Pt (0.2V).[11] The electrochemically active surface area (ECSA) of the catalysts, estimated from the cyclic voltammograms (oxygen reduction), are 1.030, 1.442 and 0.671 cm^2 for Pd/FLG, Pd/C and Pt/C respectively (SI). The polarization curves, the kinetic current densities (j_k) - calculated using the Koutechy-Levich equation[27] and the Tafel plots of the mass transport corrected kinetic current (j_k) at 1600 rpm for three catalysts, are presented in Fig. 3 (different rotation rate, SI). The Pd/FLG catalyst exhibits a positive shift of the half-wave potential by 50 mV compare to Pd/C and Pt/C catalyst showing an important improvement of the reaction kinetic. The intrinsic activities of catalysts, calculated by considering the ECSA measurements (j_{area}) and mass factor clearly demonstrate the superior performance of the Pd/FLG catalyst.

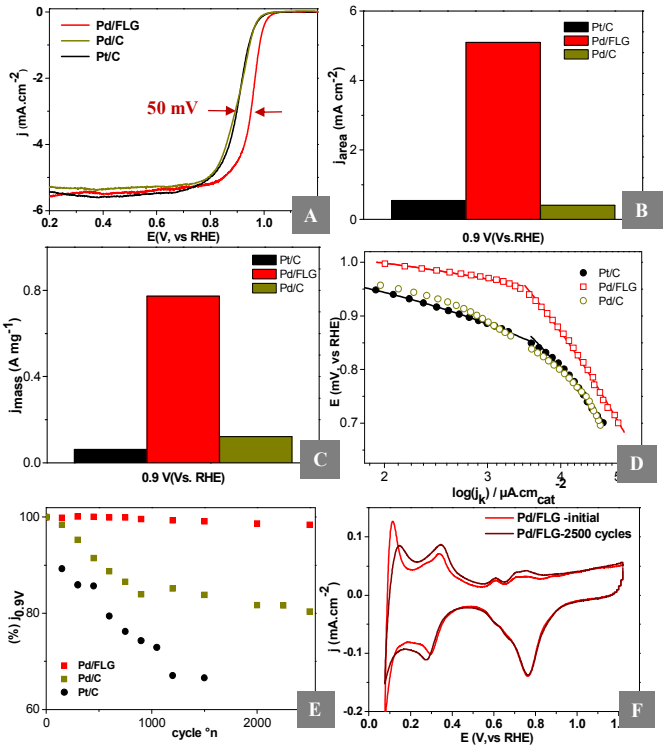

Figure 3. ORR performance of Pd/FLG (vs. Pt/C and Pd/C): (A) Polarization curves (B) ECSAs- and (C) Mass-normalized current densities (j_{area}, j_{mass}) at 1600 rpm, (D) Tafel plots, (E) Pd/FLG, Pd/C and Pt/C current density drop at 0.9V with cycles n°, (F) ECSAs measurements- CV curves of Pd/FLG before and after 2500 cycles.

The calculated kinetic currents density (j_{area}) at ~0.9V is more than 9 and 12 times higher, while mass normalized kinetic current density (j_{mass}) is 12 and 6 times higher for Pd compare to Pt/C and Pd/C, respectively. A rough estimation of Tafel slops for Pt/C (Pd/C) gives the values of ~ 58 (62) mV/dec for potential region > 0.85V and ~ 122 (130) mV/dec for region < 0.85V. In the case of Pd/FLG, the Tafel slops are curiously much lower and higher, i.e. ~ 32 mV/dec for region > 0.96V and ~ 169 mV/dec for potentials < 0.96V, respectively.

The Pd/FLG also exhibits superior performance than Pt/C and Pd/C in a long-term experiment (Fig. 3). After 2500 cycles performed at 25°C between 0.8 to 1.2V vs. RHE at 100 mV/s rate, the active surface area (ECSA) remains almost unchanged (1.02 vs. 1.03 cm^2) and only 2% drop of J_{area} is detected for Pd, while J_{area} for Pt is reduced by 35% and, for C supported Pd, by 20%.

The ORR activity of Pd/FLG in the presence of methanol drops only slightly (> 0.2M MeOH), while an important deactivation of Pd/C and even more significant of Pt/C catalyst is observed (SI).

Additional ORR tests performed in H_2SO_4 agree with literature data and uncover low Pd/FLG activity in acid medium (lower than Pt/C) (SI).

Current work is underway to define either the morphological or (and) electronic properties of Pd/FLG have an impact on ORR activity and stability performance. Both factors, related to each other, are of primary importance, as both are inseparably altered by FLG support. The flattening of the Pd particles indicates that Pd exposes high number of atoms to interact with graphene support, which can induces the modification of Pd electronic structure, while the observed specific Pd morphology seems to clearly play a role. Despite the significant dispersion of "standard shaped" Pd nanoparticles in the Pd/C and related to this high active surface, the Pd/C ORR performance is far behind. The electronic modification of the firsts Pd layers by FLG support can consist of electron transfer or charge redistribution through hybridization of their states (ligand effect) and /or to compressive/tensile strain of Pd lattice in a similar manner to crystal metals alloys[11,18] or to pseudomorphic Pd monolayers formed on various noble metals reported by Kibler et al.,[10] or to the Co_3O_4-N-graphene interface formation.[23] In the case of FLG however, a π-electrons rich structure (d-free) plays the first fiddle in the interaction with metal, introducing additionally high electrical conductivity.

Conclusions

In summary we have reported that the Pd/FLG exhibits a highest ORR performance among the monometallic family catalysts in alkaline medium. Apart from the high catalytic performance; the simple, scalable, low-cost and environment friendly preparation of the support and the catalyst render it among the most promising electrocatalysts for fuel cell applications. Detailed investigations of Pd/FLG (electronic) structure - ORR performance relationship are undergoing.

Notes and references

[a] Institut de Chimie et Procédés pour l'Énergie, l'Environnement et la Santé (ICPEES), CNRS UMR 7515-University of Strasbourg, 25 rue Becquerel 67087 Strasbourg, France
[b] Institut de Physique et Chimie des Matériaux de Strasbourg, CNRS UMR 7504, University of Strasbourg, 23 rue du Loess BP 43, 67034 STRASBOURG Cedex 2 France

*Corresponding author e-mail: janowskai@unistra.fr

Electronic Supplementary Information (ESI) available: Experimental and characterization details including catalyst preparation, TEM, AFM, SEM, XRD and electrochemical data. See DOI: 10.1039/c000000x/

Acknowledgements: Conectus program (Alsace region) is acknowledged for supporting this work. Prof. E. R. Savinova (ICPEES) is acknowledged for providing electrochemical setup facilities. Dr. Thierry Dintzer and Driss Ihiawakrim are acknowledged for a technical help during SEM/TEM analysis.

1 S. Guo, S. Zhang, S. Sun, *Angew. Chem. Int. Ed.,* 2013, **52**, 8526.
2 C. Zhang, S. Y. Hwang, A.Trout, Z. Peng, *J. Am. Chem. Soc.*, 2014, **136**,7805.
3 M. Shao, *J. Power Sources*, 2011, **196**, 2433.
4 S. Kondo, M. Nakamura, M. Norihiti, N. Hoshi, *J. Phys.Chem.C*, 2009, **113**, 12625.
5 M. Shao, T. Yu, J. H. Odell, M. Jin, Y. Xia, *Chem.Commun.*, 2011, **47**, 6566.
6 A. Anastasopoulos, J. C. Davies, L. Hannah, B. E. Hayden, C. E. Lee, C. Milhano, C. Mormiche, L. Offin, *ChemSucChem*, 2013, **6**, 1973.
7 L. Xiao, L. Zhuang, Y. Liu, J. Lu, H. D. Abruña, *J.Am.Chem.Soc*., 2009, **131**, 602.8 F. H. B. Lima, J. Zhang, M. H. Shao, B. Sasaki, E. A. Vukmirovic, R. R. Adzic, *J. Phys. Chem. C*, 2007, **111**, 404.
9 B. Hammer, J. K. Nørskov, *Surf. Sci*, 1995, **343**, 211.
10 L. A. Kibler, A. M. El-Aziz, R. Hoyer, D. M. Kolb, *Angew.Chem. Int. Ed.*, 2005, **44**, 2080.
11 M. Arenz, T. J. Schmidt, K. Wandelt, P. N. Ross, N. M. Markovic, *J. Phys. Chem. B*, 2003, **107**, 9813.
12 M. H. Shao, T. Huang, P. Liu, K. Zhang, K. Sasaki, M. B. Vucmirovic, R. R. Adzic, *Langmuir*, 2006, **22,** 10409.
13 M.-H. Shao, K. Sasaki, R. R. Adzic, *J. Am.Chem.So*., 2006, **128**, 3526.
14 J. X. Wang, H. Inada, L. Wu, Y. Zhu, Y. M. Choi, P. Liu, W.-P. Zhou, R. R. Adzic, *J. Am. Chem. Soc.*, 2009, **131**, 17298.
15 J. Zhang, F. H. B. Lima, M. H. Shao, K. Sasaki, J.X. Wang, J. Hanson, R. R. Adzic, *J.Phys. Chem.B.,* 2005, **109**, 22701.
16 Y. Zhang, Y.-C. Hsieh, V. Volkov, D. Su, W. An, R. Si, Y. Zhu, P. Liu, J. X. Wang, R. R. Adzic, *ACS Catal.*, 2014, **4**, 738.
17 L. Zhang, R. Iyyamperumal, D. F. Yancey, R. M. Crooks, G. Henkelman, *ACS Nano*, 2013, **7**, 9168.
18 P. P. Wells, E. M. Crabb, C. R. King, R. Wiltshire, B. Billsborrow, D. Thompsettd, A. E. Russell, *Phys. Chem. Chem. Phys*., 2009, **11**, 5773.
19 R. Kou, Y. Shao, D.; Wang, M. H. Engelhard, J. H. Kwak, J. Wang, V. V. Viswanathan, C. Wang, Y. Lin, Y. Wang, I. A. Aksay, J. Liu, *J. Electrochem. Commun*, 2009, **11**, 954.
20 Y. Shao, S. Zhang, C. Wang, Z. Nie J. Liu, Y. Wang, Y. Lin, *J. Power Sources*, 2010, **195**, 4600.
21 S. Guo, S. Sun, *J. Am. Chem. Soc.*, 2012, **134**, 2492.

22 Y. Liang, Y. Li, H. Wang, J. Zhou, J. Wang, T. Regier, H. Dai, *Nature Mat.* 2011, **10**, 780.
23 C. Zhang, R. Hao, H. Yin, F. Liu, Y. Hou, Nanoscale, 2012, **4**, 7326.
24 I. Janowska, F. Vigneron, O. Ersen, D. Bégin, P. Bernhardt, T. Romero, M.-J. Ledoux, C. Pham-Huu, *Carbon*, 2012, **50**, 3106.
25 I. Janowska, D. Bégin, K. Chizari, O. Ersen, P. Bernhardt, T. Romero, M.–J. Ledoux, C. Pham-Huu, *France No. 10-02719 (2010), PCT/FR2010/000730.*
26 I. Janowska, M.-S. Moldovan, O. Ersen, H. Bulou, K. Chizari, M.-J. Ledoux, C. Pham-Huu, *Nano Resaearch,* 2011, **4**, 511.
27 S. Wang, D. Yu, L. Dai, *J.Am. Chem. Soc.*, 2011, **133**, 5182.